Author Manuscript

Author Manuscript

Author Manuscript

Author Manuscript

HHS Public Access

Author manuscript

Nature. Author manuscript; available in PMC 2016 January 21.

Published in final edited form as:

Nature. 2009 May 21; 459(7245): 387–392. doi:10.1038/nature08040.

Bmi1 regulates mitochondrial function and the DNA damage response pathway

Jie Liu[#1], **Liu Cao**[#1], **Jichun Chen**[2], **Shiwei Song**[1], **In Hye Lee**[1], **Celia Quijano**[1], **Hongjun Liu**[1], **Keyvan Keyvanfar**[2], **Haoqian Chen**[1], **Long-Yue Cao**[1], **Bong-Hyun Ahn**[1], **Neil G. Kumar**[1,3], **Ilsa I. Rovira**[1], **Xiao-Ling Xu**[4], **Maarten van Lohuizen**[5], **Noboru Motoyama**[6], **Chu-Xia Deng**[4], and **Toren Finkel**[1]

[1]Translational Medicine Branch, National Heart Lung and Blood Institute, National Institutes of Health, Bethesda, Maryland 20892, USA. [2]Hematology Branch, National Heart Lung and Blood Institute, National Institutes of Health, Bethesda, Maryland 20892, USA. [3]Howard Hughes Medical Institute, NIH Research Scholar Program, Bethesda, Maryland 20892, USA. [4]Genetics of Development and Disease Branch, National Institute of Diabetes and Digestive and Kidney Disease, National Institutes of Health, Bethesda, Maryland 20892, USA. [5]Division of Molecular Genetics, Netherlands Cancer Institute and Centre for Biomedical Genetics, 1066 CX Amsterdam, The Netherlands. [6]Department of Geriatric Medicine, National Institute for Longevity Sciences National Center for Geriatrics and Gerontology 36-3, Gengo, Morioka, Obu, Aichi 474-8522, Japan.

[#] These authors contributed equally to this work.

Abstract

Mice deficient in the Polycomb repressor Bmi1 develop numerous abnormalities including a severe defect in stem cell self-renewal, alterations in thymocyte maturation and a shortened lifespan. Previous work has implicated de-repression of the *Ink4a/Arf* (also known as *Cdkn2a*) locus as mediating many of the aspects of the *Bmi1*$^{-/-}$ phenotype. Here we demonstrate that cells derived from *Bmi1*$^{-/-}$ mice also have impaired mitochondrial function, a marked increase in the intracellular levels of reactive oxygen species and subsequent engagement of the DNA damage response pathway. Furthermore, many of the deficiencies normally observed in *Bmi1*$^{-/-}$ mice improve after either pharmacological treatment with the antioxidant *N*-acetylcysteine or genetic disruption of the DNA damage response pathway by Chk2 (also known as Chek2) deletion. These results demonstrate that Bmi1 has an unexpected role in maintaining mitochondrial function and redox homeostasis and indicate that the Polycomb family of proteins can coordinately regulate cellular metabolism with stem and progenitor cell function.

Author Information Reprints and permissions information is available at www.nature.com/reprints. Correspondence and requests for materials should be addressed to T.F. (finkelt@nih.gov) or L.C. (Liu.Cao@nih.gov)..

Full Methods and any associated references are available in the online version of the paper at www.nature.com/nature.

Supplementary Information is linked to the online version of the paper at www.nature.com/nature.

Author Manuscript Author Manuscript Author Manuscript Author Manuscript

Bmi1 is a member of the Polycomb family of transcriptional repressors that mediate gene silencing by regulating chromatin structure and is essential for the maintenance and self-renewal of both haematopoietic and neural stem cells[1,2]. Mice deficient in Bmi1 have a number of defects including severe neurological abnormalities, alterations in various haematopoietic cell lineages, a generalized failure-to-thrive and a markedly shortened lifespan. Previous studies have documented that approximately 50% of the knockout mice die before the completion of weaning and the remaining 50% succumb anywhere from 3 to 20 weeks of age[3]. In an effort to understand how the effects of Bmi1 are mediated, significant attention has been placed on the repression of the *Ink4a/Arf* locus, which encodes two separate tumour suppressors and cell cycle regulators, $p16^{Ink4a}$ and $p19^{Arf}$ (refs 4–7). The importance of the transcriptional repression of the *Ink4a/Arf* locus is underscored by the observation that mice deficient in Bmi1 and also lacking $p16^{Ink4a}$, $p19^{Arf}$ or both of these gene products develop less severe neurological and haematological abnormalities than $Bmi1^{-/-}$ animals[4–6].

Although improved, mice lacking Bmi1 as well as Ink4a/Arf remain significantly smaller than wild-type littermates and their overall survival is similar to that of $Bmi1^{-/-}$ mice[6]. In addition, examination of the number of peripheral nucleated thymocytes or splenocytes, as well as the cellular composition of the bone marrow microenvironment itself, remains significantly altered in combined Bmi1/Ink4a/Arf-deficient mice[8]. These results therefore indicate that, besides repression of the *Ink4a/Arf* locus, additional Bmi1-regulated pathways undoubtedly exist. Here we demonstrate that Bmi1 can separately regulate mitochondrial function, reactive oxygen species (ROS) levels and the activation of the DNA damage response (DDR) pathway.

Bmi1 regulates ROS levels

Mice deficient in either the ataxia telangiectasia mutated (Atm) gene product or the FOXO family of transcription factors demonstrate a rapid postnatal decline in haematopoietic stem cell (HSC) number that in each case is associated with a rise in ROS levels within the c-$KIT^1Sca\text{-}1^1Lin^-$ (LSK) bone marrow cell population that includes HSCs[9,10]. We therefore sought to test whether a similar rise in ROS levels was evident in $Bmi1^{-/-}$ cells. Assessment of unfractionated bone marrow, purified LSK cells and bone marrow cells expressing SLAM family receptors previously shown to allow for enrichment of long-term HSC cells (LT-HSCs)[11] demonstrated that the absence of $Bmi1^{-/-}$ resulted in increased levels of ROS (Fig. 1a and Supplementary Fig. 1). A similar increase in ROS levels was also evident in various other cell types known to be impaired in $Bmi1^{-/-}$ mice, including freshly isolated thymocytes (Fig. 1b and Supplementary Fig. 1).

In an effort to explain this observed rise in ROS, we made use of several previous gene expression studies that have identified a multitude of Polycomb target genes[1,12,13]. Among these identified targets were numerous genes either involved directly in ROS generation or that localize to the mitochondria and are known to affect mitochondrial function. Given the scarcity of LT-HSCs in $Bmi1^{-/-}$ mice, we chose to analyse gene expression in $Bmi1^{-/-}$ thymocytes, because previous reports have demonstrated a marked perturbation of this cell population in Bmi1-deficient mice[3,4] and our data indicated that these cells had marked

Author Manuscript Author Manuscript Author Manuscript Author Manuscript

differences in ROS levels. As noted in Fig. 1c, *Bmi1*$^{-/-}$ thymoctyes de-repressed a number of previously identified Polycomb-regulated gene products that can regulate intracellular redox homeostasis. Given that mitochondria can produce oxidants and are in turn quite sensitive to their damaging effects[14], we sought to analyse the mitochondrial function of *Bmi1*$^{-/-}$ cells. Intact *Bmi1*$^{-/-}$ thymocytes had both reduced basal mitochondrial oxygen consumption and reduced mitochondrial oxidative capacity (Fig. 1d). Basal ATP levels were also significantly reduced in *Bmi1*$^{-/-}$ thymocytes (Fig. 1e) as well as in other tissues (Supplementary Fig. 2). The observed differences in mitochondrial respiration and intracellular energetics were not however accompanied by any obvious differences in mitochondrial number, structure, bio-genesis or rate of degradation (Supplementary Fig. 3).

Consistent with our intact cellular respiration measurements, we observed significant impairment in the function of purified *Bmi1*$^{-/-}$ mitochondria (Fig. 1f, g). The interruption of flow down the electron transport chain (ETC) evident in *Bmi1*$^{-/-}$ mitochondria is believed to be a major source for ROS generation. Impaired electron flow increases the likelihood of superoxide formation and is often accompanied by a build-up of mitochondrial reducing equivalents (for example, NADH). Consistent with such a mechanism, NAD(P)H levels were increased in *Bmi1*$^{-/-}$ thymocytes (Fig. 1h). To substantiate further the connection between Polycomb activity, mitochondrial function and oxidant stress, we next measured ROS levels in the setting of various inhibitors of mitochondrial function. As expected, using the complex I inhibitor rotenone to reduce electron flow increased ROS levels (Fig. 1i). In contrast, treatment with the pharmacological uncoupler FCCP, which specifically lowers mitochondrial membrane potential and hence augments ETC flux, markedly reduced ROS levels in *Bmi1*$^{-/-}$cells. Consistent with the observed rise in Duox1 and Duox2 expression (Fig. 1c), we also observed a small but non-significant decrease in ROS levels after treatment with the NADPH oxidase inhibitor DPI (Fig. 1i). Finally, the use of the mitochondrial redox fluorophore MitoSox Red provided additional support for the hypothesis that the mitochondria are the major source of increased ROS levels observed in *Bmi1*$^{-/-}$ cells (Fig. 1j and Supplementary Fig. 3).

Antioxidants can rescue *Bmi1*$^{-/-}$ mice

We next sought to assess whether the increase in ROS levels might contribute to the various *in vivo* phenotypic defects observed in *Bmi1*$^{-/-}$ mice. We randomizedfour-week-old *Bmi1*$^{-/-}$ mice to treatment with and without the antioxidant scavenger *N*-acetylcysteine (NAC). After one week of treatment, ROS levels in *Bmi1*$^{-/-}$ thymocytes had been reduced to near wild-type levels (Fig. 2a). Coincident with this reduction, we noted a marked increase in the overall size of the thymus in the antioxidant-treated *Bmi1*$^{-/-}$ mice (Fig. 2b). This increase in thymus size was also accompanied by a significant increase in the overall number of total thymocytes in the antioxidant-treated *Bmi1*$^{-/-}$ animals, although *Bmi1*$^{-/-}$ mice treated with NAC still had reduced number of thymocytes when compared to wild-type animals (Fig. 2c). Previous studies have also demonstrated that *Bmi1*$^{-/-}$ mice also have defects in thymocyte maturation[3,4]. As noted in Fig. 2d, approximately 80% of cells isolated from wild-type mice were $CD4^+CD8^+$ double-positive thymocytes. A one-week administration of NAC to wild-type mice did not appreciably alter this distribution. In contrast, the frequency of $CD4^+CD8^+$ double-positive thymocytes observed in untreated Bmi1$^{-/-}$ mice was

Author Manuscript Author Manuscript Author Manuscript Author Manuscript

markedly reduced, yet normalized after NAC administration (Fig. 2d, e). Finally, NAC administration had effects beyond altering thymocyte function, because this intervention also appeared to partially correct the failure-to-thrive phenotype seen in *Bmi1*$^{-/-}$ animals (Fig. 2f).

Quantitative real-time polymerase chain reaction (rtPCR) analysis demonstrated that the improvement seen in *Bmi1*$^{-/-}$ mice after antioxidant treatment was not accompanied by any apparent alteration in *Ink4a/Arf* transcription (Fig. 3a). Thus, the Bmi1-mediated rise in ROS does not seem to be required for the subsequent induction of Ink4a/Arf. There is evidence that, in certain situations, a rise in p16^{Ink4a} expression can be associated with, and appears to be required for, a subsequent increase in oxidant levels[15]. Thus, it seemed possible that NAC was rescuing *Bmi1*$^{-/-}$ mice by scavenging oxidants that were produced as a result of p16^{Ink4a} expression. To test this possibility formally, we analysed the levels of ROS in thymocytes obtained from *Bmi1*$^{-/-}$ mice or from mice doubly deficient in both *Bmi1* and *p16*^{Ink4a} (Fig. 3b and Supplementary Fig. 4). The induction of p16^{Ink4a} does not seem to be required for the rise in ROS levels observed in *Bmi1*$^{-/-}$ cells.

Bmi1 regulates the DDR pathway

To understand which other pathways might be activated by the observed increase in ROS levels, we took advantage of previous observations demonstrating that oxidative stress can trigger activation of the DDR pathway[16]. As noted in Fig. 3c, *Bmi1*$^{-/-}$ thymocytes had increased levels of 8-oxoguanine, a stable marker of oxidatively damaged DNA. In addition, consistent with ongoing DNA damage, we observed increased nuclear foci of 53BP1 (also known as Trp53bp1), another known hallmark of DNA damage and DDR activation[17]. In *Bmi1*$^{-/-}$ mice treated with NAC for one week before collection, the number of 53BP1 nuclear foci was markedly reduced (Fig. 3d). Other DDR components including Chk2 were also activated in *Bmi1*$^{-/-}$ cells, and again this activation was reduced by antioxidant treatment (Fig. 3e). These results indicate that the sustained levels of ROS seen in *Bmi1*$^{-/-}$ mice are sufficient to damage DNA directly and to engage the DDR pathway. To underscore this point further, we observed that treatment of thymocytes with exogenous hydrogen peroxide could activate the DDR pathway and that cells obtained from *Chk2*$^{-/-}$ mice were largely protected from ROS-induced cell death (Supplementary Fig. 5). These results indicated that interruption of the DDR pathway by deletion of Chk2 may provide some benefit to the oxidatively stressed *Bmi1*$^{-/-}$ cells and tissues. To begin to address this hypothesis formally, we assessed the survival in culture of wild-type, *Chk2*$^{-/-}$, *Bmi1*$^{-/-}$ or combined *Bmi1*$^{-/-}$*Chk2*$^{-/-}$ thymocytes. Whereas *Bmi1*$^{-/-}$ thymocytes rapidly lost viability in culture, the survival of thymocytes lacking both Bmi1 and Chk2 was similar to that in wild-type cells (Fig. 3f). A similar rescue of *Bmi1*$^{-/-}$ thymocytes could also be obtained by supplementing the media with NAC (Supplementary Fig. 6).

Chk2 deletion rescues *Bmi1*$^{-/-}$ mice

To understand further how the activation of the DDR pathway might contribute to the overall *Bmi1*$^{-/-}$ phenotype, we asked whether mice lacking both Bmi1 and Chk2 demonstrated any phenotypic improvement compared to *Bmi1*$^{-/-}$ mice. Previous results have

Author Manuscript Author Manuscript Author Manuscript Author Manuscript

demonstrated that, whereas Chk2-deficient cells have an increase in radioresistance, *Chk2*$^{-/-}$ mice do not exhibit a high rate of spontaneous tumour formation and appear, for the most part, to be phenotypically identical to wild-type mice[18,19]. We first examined *in vivo* thymocyte maturation in either *Bmi1*$^{-/-}$ or combined *Bmi1*$^{-/-}$*Chk2*$^{-/-}$ animals. As previously noted with antioxidant treatment, the overall size of the thymus, as well as the spleen, was significantly larger in the *Bmi1*$^{-/-}$*Chk2*$^{-/-}$ mice than in *Bmi1*$^{-/-}$-only mice (Supplementary Fig. 7). Similarly, the previously observed reduction in the number of $CD4^+CD8^+$ double-positive thymocytes in *Bmi1*$^{-/-}$ mice was significantly less marked in mice lacking both *Bmi1* and *Chk2* (Fig. 4a). We also noted significant alterations in the overall architecture of the thymus. In contrast to wild-type mice, *Bmi1*$^{-/-}$ mice lacked a distinct separation between thymic cortex and medulla (Fig. 4b). A similar change in overall thymus architecture has been noted in other animal models with impaired thymocyte maturation[20,21]. In contrast, a near normal compartmentalization of thymic cortex and medulla was observed in the *Bmi1*$^{-/-}$*Chk2*$^{-/-}$ mice (Fig. 4b). Given that *Chk2* deletion seems to protect thymocytes from ROS-mediated cell death (Fig. 3f and Supplementary Fig. 5), we postulated that the absence of Chk2 could be rescuing thymocyte number and maturation by inhibiting apoptosis. Consistent with this notion, levels of apoptosis were increased in the cortex of *Bmi1*$^{-/-}$ compared to wild-type animals, whereas this level of overall apoptosis was reduced in animals deficient in both *Bmi1* and *Chk2* (Fig. 4c). As previously observed with antioxidant treatment, the improvement observed in the *Bmi1*$^{-/-}$*Chk2*$^{-/-}$ mice did not seem to be the result of alterations in the induction of the *Ink4a/Arf* locus (Fig. 4d and Supplementary Fig. 8). Similarly, deletion of *Chk2* did not directly alter the level of ROS induced by the absence of Bmi1 expression (Supplementary Fig. 9). Interestingly, the combination of NAC treatment and *Chk2* deletion was slightly more effective at rescuing *Bmi1*$^{-/-}$ thymocyte number and maturation than *Chk2* deletion alone, indicating that some of the effects of ROS may be independent of the DDR response (Supplementary Fig. 10).

We next assessed whether the absence of Chk2 could also improve the number or functional capacity of *Bmi1*$^{-/-}$ haematopoietic stem or progenitor cells. To begin to address this issue, we measured the number of LSK cells in either *Bmi1*$^{-/-}$ or combined *Bmi1*$^{-/-}$*Chk2*$^{-/-}$ mice. This cell population is generally believed to contain abundant progenitor cells, as well as rarer, long-term repopulating cells. As noted in Fig. 4e, the number of LSK cells in mice lacking both *Bmi1* and *Chk2* was significantly higher than that seen in *Bmi1*$^{-/-}$ animals. We next sought to assess the functional capacity of the progenitor cells isolated from *Bmi1*$^{-/-}$*Chk2*$^{-/-}$ mice. Bone marrow cells from *Bmi1*$^{-/-}$ mice were markedly impaired in their *in vitro* colony-forming ability whereas the colony-forming capacity of *Bmi1*$^{-/-}$*Chk2*$^{-/-}$ bone marrow cells was significantly improved (Supplementary Fig. 11). In a further *in vivo* test of progenitor function, we measured spleen colony-forming units (CFU-S) that formed after injection of total bone marrow (1×10^5 cells) into irradiated hosts. Again, using this *in vivo* test of progenitor cell function, we noted a marked impairment of *Bmi1*$^{-/-}$ bone marrow that was significantly less pronounced in the *Bmi1*$^{-/-}$*Chk2*$^{-/-}$ mice (Fig. 4f).

Although these results indicate that *Chk2* deletion results in improvement in the number and function of *Bmi1*$^{-/-}$ progenitor cells, they do not address whetherthere is also a concomitant improvement in long-term repopulating ability. To test this, we performed competitive

Author Manuscript Author Manuscript Author Manuscript Author Manuscript

repopulation studies using wild-type, *Bmi1*$^{-/-}$, *Bmi1*$^{+/-}$ or combined *Bmi1*$^{-/-}$*Chk2*$^{-/-}$ bone marrow. As previously reported[1,8], consistent with a defect in stem cell maintenance and self-renewal, we observed that *Bmi1*$^{-/-}$ bone marrow was unable to contribute in such long-term repopulation assays (Supplementary Fig. 12). We also observed essentially no contribution to long-term repopulation from the *Bmi1*$^{-/-}$*Chk2*$^{-/-}$ bone marrow (Fig. 4g and Supplementary Fig. 12). We therefore conclude that, whereas *Bmi1*$^{-/-}$*Chk2*$^{-/-}$ mice have an increased number of LSK cells and an apparent improvement in progenitor cell function, deletion of *Chk2* does not rescue the self-renewal defect seen in *Bmi1*$^{-/-}$ mice.

The improvement in *Bmi1*$^{-/-}$ mice that was observed by concomitant deletion of *Chk2* extended beyond thymocytes and haematopoietic progenitors. Indeed, the overall appearance of these doubly deficient mice was improved compared to the *Bmi1*$^{-/-}$ animals (Fig. 4h). This was also accompanied by a significant increase in overall body weight (Fig. 4i). In addition, whereas the *Bmi1*$^{-/-}$ mice had a severe ataxia, this phenotype also appeared to be mitigated in the *Bmi1*$^{-/-}$*Chk2*$^{-/-}$ animals. Consistent with such improvement, the cerebellum of the double-deficient mice showed a marked increase in cellularity and was more developed than what was observed in *Bmi1*$^{-/-}$ mice (Fig. 4j). Similarly, whereas *Bmi1*$^{-/-}$ mice were infertile, both male and female combined *Bmi1*$^{-/-}$*Chk2*$^{-/-}$ mice were capable of generating viable offspring. In contrast, the deletion of *Chk2* did not rescue previously described changes in the axial skeleton, because we observed that approximately 80% of the *Bmi1*$^{-/-}$*Chk2*$^{-/-}$ mice had 6 as opposed to the normal 7 vertebrosternal ribs[3].

Finally, we noted a number of progeriod features in the *Bmi1*$^{-/-}$ mice that were largely absent in age-matched *Bmi1*$^{-/-}$*Chk2*$^{-/-}$ mice (Supplementary Fig. 13). On the basis of these observations, we asked whether the absence of Chk2 could extend the median and maximum lifespan of animals lacking Bmi1. In our colony, the median survival of *Bmi1*$^{-/-}$ mice was roughly 1 month and essentially all mice succumbed by 3–4 months (Fig. 4k). Deletion of one copy of *Chk2* provided a survival advantage, whereas deletion of both copies of *Chk2* was even more effective and extended the median survival of the *Bmi1*$^{-/-}$*Chk2*$^{-/-}$ mice to approximately 6 months.

Conclusions

We demonstrate that the absence of Bmi1 leads to increased expression of a collection of gene products involved in mitochondrial function and ROS homeostasis. Cells lacking Bmi1 have significant mitochondrial dysfunction accompanied by a sustained increase in ROS that is sufficient to engage the DDR pathway. Treatment with an antioxidant or interruption of the DDR by *Chk2* deletion substantially improves some, but not all, aspects of the *Bmi1*$^{-/-}$ mice. Our observations further indicate that, in *Bmi1*$^{-/-}$ mice, ROS act independently of the Ink4a/Arf pathway. In addition, although in the context of the *Bmi1*$^{-/-}$ mouse deletion of the *Ink4a/Arf* locus results in substantial rescue of the LT-HSC defect, it is interesting to note that the beneficial effects of *Chk2* deletion are exclusively confined to very early haematopoietic progenitor cells.

Activation of the DDR response has been invoked as a natural consequence of age-associated damage. For instance, when compared to younger HSCs, purified HSCs from old

Author Manuscript Author Manuscript Author Manuscript Author Manuscript

mice demonstrate increased levels of γ-H2AX nuclear foci—a marker of DNA damage[22]. Although such old HSCs do not decline in absolute number, the activation of the DDR does correlate with impairment of stem cell function. Similarly, in a number of mouse genetic models in which there are inherited defects in various components of the DNA repair apparatus, there is also evidence for a reduction in functional capacity of transplanted HSCs[23,24]. In addition, recent evidence indicates that the self-renewal of cancer stem cells can also be limited by oncogene-induced DNA damage[25]. In other animal models, the age-dependent increase in $p16^{Ink4a}$ expression has been linked to age-dependent decline in stem cell function[26]. Furthermore, in several independent models, deletion of *p16*^{Ink4a} leads to improved functional capacity of neural, pancreatic and haematopoietic stem cells[27–29]. Thus, both the DDR pathway and a rise in $p16^{Ink4a}$ have been linked to stem and progenitor cell ageing and dysfunction. Outside of the stem and progenitor compartment, both activation of the Ink4a/Arf locus and engagement of the DDR pathway have also been separately implicated in mediating cellular senescence, growth arrest and/or cell death induced by various stresses[30,31]. Activation of these two pathways has been invoked as an important tumour suppressor barrier, because both pathways act as potent inhibitors of the proliferation or propagation of damaged cells. Interestingly, our data indicate that the absence of Bmi1 results in the simultaneous engagement of both of these stress-activated and tumour-suppressive pathways and that both of these pathways appear to separately contribute to the overall phenotype of the *Bmi1*$^{-/-}$ mice (Fig. 4l). Furthermore, the necessity of stem cells to persist throughout the entire lifespan of the organism indicates that these cells might have particularly stringent requirements to limit ROS production. Our results imply that the Polycomb family of proteins might be uniquely positioned to coordinately regulate mitochondrial function and redox homeostasis with overall stem cell biology.

METHODS

Cells and mice

Bmi1$^{+/-}$ and *Chk2*$^{+/-}$ mice have been described previously[3,18]. *Bmi1*$^{+/-}$ C57BL/6 mice and *Chk2*$^{+/-}$mice on a mixed 129/Black Swiss genetic background were crossed to generate *Bmi1*$^{+/+}$ and *Bmi1*$^{-/-}$ mice with various Chk2 status. Littermate controls were used for analysis and all mice were geno-typed routinely by PCR with mouse tail DNA. Except where indicated, histological and biological analysis was performed for both male and female mice at 1–3 months of age. Mice deleted specifically for *p16*^{Ink4a} have been described[35] and were obtained from the National Cancer Institute (MMHCC repository, Fredrick MD). For the *in vivo* administration of NAC, we randomized animals to normal drinking water, or water containing NAC at 1 mg ml^{-1} as previously described[10]. In addition, owing to the overall frailty of *Bmi1*$^{-/-}$ mice, the food of animals treated or untreated with antioxidant was soaked in NAC-treated or -untreated drinking water and placed inside the cage.

Intracellular ROS analysis

Total bone marrow cells, LSK cells and cells stained for SLAM family members (CD150 and CD48; BioLegend) as well as CD41 (BioLegend) were isolated as previously described[11,36]. In general, thymocytes and splenocytes were isolated from 6–8-week-old

Author Manuscript Author Manuscript Author Manuscript Author Manuscript

mice and were plated at an initial density of 1×10^6 cells per ml in Dulbecco Modified Essential Medium (DMEM) supplemented with 10% fetal bovine serum. Thymocyte populations were analysed where indicated by CD4 and CD8 staining (BD Biosciences). For analysis of intracellular ROS, bone marrow cells enriched for LT-HSCs, thymocytes and other cell types were incubated with 5 μM DCFDA (Invitrogen) and placed in a shaker at 37 °C for 30 min, followed immediately by flow cytometry analysis using an LSRII instrument (Becton-Dickinson). Viable cells (1×10^6) as determined by 7-AAD staining were used for the analysis of ROS levels. Where indicated, cells were treated with either rotenone, carbonyl cyanide p-trifluor-methoxyphenylhydrazone (FCCP) or diphenyleneiodonium chloride (DPI) for 10 min before assessment of ROS levels.

Mitochondrial isolation, functional studies and ATP determination

For isolation of functional mitochondria from mouse tissues, we rapidly collected, washed and minced mouse hearts in ice-cold Isolation Buffer I containing 210 mM mannitol, 70 mM sucrose, 5 mM HEPES (pH 7.4), 1 mM EGTA and 0.5 mg ml^{-1} BSA. The hearts were then homogenized in this buffer with a glass-Teflon motorized homogenizer. The mitochondrial fraction was isolated by differential centrifugation and subsequently washed twice before resuspension in Isolation Buffer I at a concentration of 0.5 mg ml^{-1} before functional assessment.

Mitochondrial respiration from intact mitochondria was measured by standard protocols using a respiration buffer containing 225 mM mannitol, 75 mM sucrose, 10 mM KCl, 10 mM Tris-HCl and 5 mM KH_2PO_4 at pH 7.2. Glutamate (5 mM), malate (5 mM) and ADP (1 mM) were used to assay respiration through complex I. Succinate (5 mM), rotenone (1 μM) and ADP (1 mM) were used to assay complex II respiration. Respiratory control ratios (RCRs; state 3/state 4) were determined after inhibition of mitochondrial ATPase with oligomycin. Measurement of intact cellular respiration was performed using the Seahorse XF24 analyser[32]. Respiration was measured under basal condition, in the presence of the mitochondrial inhibitor oligomycin (0.5 μM) and in the presence of the mitochondrial uncoupler FCCP (1 μM) to assess maximal oxidative capacity as we have described previously[37].

ATP was measured using the ATP-determination kit (Molecular Probes). For *in vivo* measurements, mice tissues were rapidly collected and immediately placed in ice-cold ATP buffer (20 mM Tris, pH 7.5, 0.5% Nonidet P-40, 25 mM NaCl, 2.5 mM EDTA) for 5 min. Tissue samples then underwent one five-second round of sonication. Lysates were than centrifuged at 13,000*g* for 30 min and the supernatant measured for protein concentration. ATP concentration was measured from 0.2 μg of this protein lysate. We always measured ATP from freshly isolated (not frozen) tissues.

HSC cultures and colony-forming assays

CFU-GM *in vitro* assays were performed according to the manufacturer's instructions (StemCell Technologies). In brief, freshly isolated total bone marrow cells were cultured in semisolid MethoCult media supplemented with 10 ng ml^{-1} GM-CSF. Cells were plated in triplicate at an initial density of 2×10^4 cells per well of a 12-well plate. After 5–7 days of

Author Manuscript Author Manuscript Author Manuscript Author Manuscript

culture, CFU-GM colonies were assessed. The CFU-S assay was performed as previously described[38]. In brief, 1×10^5 bone marrow cells from five donors of each group (*Bmi1*$^{-/-}$, combined *Bmi1*$^{-/-}$*Chk2*$^{-/-}$ and wild-type controls) were transplanted into each of three 12-week-old normal B6 recipients pre-irradiated at 950 rad. Six B6 mice that received the same dose of irradiation and no subsequent bone marrow transplantation were used as negative controls. The spleens of all animals were fixed on day 12 after transplantation, and the total numbers of colonies per spleen were assessed.

For competitive repopulation experiments, lethally irradiated C57BJ/6 mice (B6-CD45.2) were competitively reconstituted with 1×10^6 total bone morrow cells from *Bmi1*$^{+/+}$, *Bmi1*$^{+/-}$, *Bmi1*$^{-/-}$ or combined Bmi1/Chk2-deficient mice. We used five recipients in each group and each recipient also received competitive repopulation with 1×10^6 bone marrow cells obtained from C57BJ/6 mice congenic for the CD45 locus (B6-CD45.1). Analysis was performed on a monthly basis after transplantation up to month four. Peripheral blood cells of the recipients were stained with antibodies against CD45.1, CD45.2, B220, CD3 and Mac-1 to monitor the reconstitution of both myeloid and lymphoid lineages.

Gene expression

Total RNA was isolated by using Trizol reagent and subsequently treated with DNase I (Invitrogen). Complementary DNA was prepared using Taqman reverse transcription reagents and oligo-dT primers. Quantitative rtPCR for *Ink4a/Arf* expression or for the expression of other Bmi1-regulated genes was performed with 50 ng cDNA on an MxP3005P real-time PCR system (Stratagene) using SYBR Green PCR Mastermix (Applied Biosystems) according to the manufacturer's instructions. For primer sequences, see Supplementary Information and Supplementary Methods.

Supplementary Material

Refer to Web version on PubMed Central for supplementary material.

Acknowledgements

We are grateful to M. Clarke for providing the initial supply of *Bmi1*$^{-/-}$ mice, to J. Moss for the gift of anti-PARP antibodies and to M. Daniels and the NHLBI electron microscope core for their assistance. This work was supported by funding from the NIH intramural program and the Ellison Medical Foundation.

References

1. Park IK, et al. Bmi-1 is required for maintenance of adult self-renewing haematopoietic stem cells. Nature. 2003; 423:302–305. [PubMed: 12714971]
2. Molofsky AV, et al. Bmi-1 dependence distinguishes neural stem cell self-renewal from progenitor proliferation. Nature. 2003; 425:962–967. [PubMed: 14574365]
3. van der Lugt NM, et al. Posterior transformation, neurological abnormalities, and severe hematopoietic defects in mice with a targeted deletion of the bmi-1 protooncogene. Genes Dev. 1994; 8:757–769. [PubMed: 7926765]
4. Jacobs JJ, Kieboom K, Marino S, DePinho RA, van Lohuizen M. The oncogene and Polycomb-group gene bmi-1 regulates cell proliferation and senescence through the ink4a locus. Nature. 1999; 397:164–168. [PubMed: 9923679]

Author Manuscript Author Manuscript Author Manuscript Author Manuscript

5. Bruggeman SW, et al. Ink4a and Arf differentially affect cell proliferation and neural stem cell self-renewal in Bmi1-deficient mice. Genes Dev. 2005; 19:1438–1443. [PubMed: 15964995]
6. Molofsky AV, He S, Bydon M, Morrison SJ, Pardal R. Bmi-1 promotes neural stem cell self-renewal and neural development but not mouse growth and survival by repressing the p16Ink4a and p19Arf senescence pathways. Genes Dev. 2005; 19:1432–1437. [PubMed: 15964994]
7. Bracken AP, et al. The Polycomb group proteins bind throughout the INK4A-ARF locus and are disassociated in senescent cells. Genes Dev. 2007; 21:525–530. [PubMed: 17344414]
8. Oguro H, et al. Differential impact of Ink4a and Arf on hematopoietic stem cells and their bone marrow microenvironment in Bmi1-deficient mice. J. Exp. Med. 2006; 203:2247–2253. [PubMed: 16954369]
9. Tothova Z, et al. FoxOs are critical mediators of hematopoietic stem cell resistance to physiologic oxidative stress. Cell. 2007; 128:325–339. [PubMed: 17254970]
10. Ito K, et al. Regulation of oxidative stress by ATM is required for self-renewal of haematopoietic stem cells. Nature. 2004; 431:997–1002. [PubMed: 15496926]
11. Kiel MJ, et al. SLAM family receptors distinguish hematopoietic stem and progenitor cells and reveal endothelial niches for stem cells. Cell. 2005; 121:1109–1121. [PubMed: 15989959]
12. Bracken AP, Dietrich N, Pasini D, Hansen KH, Helin K. Genome-wide mapping of Polycomb target genes unravels their roles in cell fate transitions. Genes Dev. 2006; 20:1123–1136. [PubMed: 16618801]
13. Fasano CA, et al. shRNA knockdown of Bmi-1 reveals a critical role for p21-Rb pathway in NSC self-renewal during development. Cell Stem Cell. 2007; 1:87–99. [PubMed: 18371338]
14. Balaban RS, Nemoto S, Finkel T. Mitochondria, oxidants, and aging. Cell. 2005; 120:483–495. [PubMed: 15734681]
15. Takahashi A, et al. Mitogenic signalling and the p16INK4a-Rb pathway cooperate to enforce irreversible cellular senescence. Nature Cell Biol. 2006; 8:1291–1297. [PubMed: 17028578]
16. Lombard DB, et al. DNA repair, genome stability, and aging. Cell. 2005; 120:497–512. [PubMed: 15734682]
17. Adams MM, Carpenter PB. Tying the loose ends together in DNA double strand break repair with 53BP1. Cell Div. 2006; 1:19. [PubMed: 16945145]
18. Takai H, et al. Chk2-deficient mice exhibit radioresistance and defective p53-mediated transcription. EMBO J. 2002; 21:5195–5205. [PubMed: 12356735]
19. Hirao A, et al. Chk2 is a tumor suppressor that regulates apoptosis in both an ataxia telangiectasia mutated (ATM)-dependent and an ATM-independent manner. Mol. Cell. Biol. 2002; 22:6521–6532. [PubMed: 12192050]
20. Okada H, et al. Survivin loss in thymocytes triggers p53-mediated growth arrest and p53-independent cell death. J. Exp. Med. 2004; 199:399–410. [PubMed: 14757745]
21. Zaugg K, et al. Cross-talk between Chk1 and Chk2 in double-mutant thymocytes. Proc. Natl Acad. Sci. USA. 2007; 104:3805–3810. [PubMed: 17360434]
22. Rossi DJ, et al. Deficiencies in DNA damage repair limit the function of haematopoietic stem cells with age. Nature. 2007; 447:725–729. [PubMed: 17554309]
23. Reese JS, Liu L, Gerson SL. Repopulating defect of mismatch repair-deficient hematopoietic stem cells. Blood. 2003; 102:1626–1633. [PubMed: 12730104]
24. Nijnik A, et al. DNA repair is limiting for haematopoietic stem cells during ageing. Nature. 2007; 447:686–690. [PubMed: 17554302]
25. Viale A, et al. Cell-cycle restriction limits DNA damage and maintains self-renewal of leukaemia stem cells. Nature. 2009; 457:51–56. [PubMed: 19122635]
26. Rossi DJ, Jamieson CH, Weissman IL. Stems cells and the pathways to aging and cancer. Cell. 2008; 132:681–696. [PubMed: 18295583]
27. Janzen V, et al. Stem-cell ageing modified by the cyclin-dependent kinase inhibitor p16INK4a. Nature. 2006; 443:421–426. [PubMed: 16957735]
28. Molofsky AV, et al. Increasing p16INK4a expression decreases forebrain progenitors and neurogenesis during ageing. Nature. 2006; 443:448–452. [PubMed: 16957738]

Author Manuscript Author Manuscript Author Manuscript Author Manuscript

29. Krishnamurthy J, et al. p16INK4a induces an age-dependent decline in islet regenerative potential. Nature. 2006; 443:453–457. [PubMed: 16957737]
30. Collado M, Blasco MA, Serrano M. Cellular senescence in cancer and aging. Cell. 2007; 130:223–233. [PubMed: 17662938]
31. Finkel T, Serrano M, Blasco MA. The common biology of cancer and ageing. Nature. 2007; 448:767–774. [PubMed: 17700693]
32. Ferrick DA, Neilson A, Beeson C. Advances in measuring cellular bioenergetics using extracellular flux. Drug Discov. Today. 2008; 13:268–274. [PubMed: 18342804]
33. Struthers L, Patel R, Clark J, Thomas S. Direct detection of 8-oxodeoxyguanosine and 8-oxoguanine by avidin and its analogues. Anal. Biochem. 1998; 255:20–31. [PubMed: 9448838]
34. Neumann CA, et al. Essential role for the peroxiredoxin Prdx1 in erythrocyte antioxidant defence and tumour suppression. Nature. 2003; 424:561–565. [PubMed: 12891360]
35. Sharpless NE, et al. Loss of p16Ink4a with retention of p19Arf predisposes mice to tumorigenesis. Nature. 2001; 413:86–91. [PubMed: 11544531]
36. Smith AL, Ellison FM, McCoy JP Jr, Chen J. c-Kit expression and stem cell factor-induced hematopoietic cell proliferation are up-regulated in aged B6D2F1 mice. J. Gerontol. A Biol. Sci. Med. Sci. 2005; 60:448–456. [PubMed: 15933382]
37. Schieke SM, et al. The mammalian target of rapamycin (mTOR) pathway regulates mitochondrial oxygen consumption and oxidative capacity. J. Biol. Chem. 2006; 281:27643–27652. [PubMed: 16847060]
38. TeKippe M, Harrison DE, Chen J. Expansion of hematopoietic stem cell phenotype and activity in Trp53-null mice. Exp. Hematol. 2003; 31:521–527. [PubMed: 12829028]

Author Manuscript Author Manuscript Author Manuscript Author Manuscript

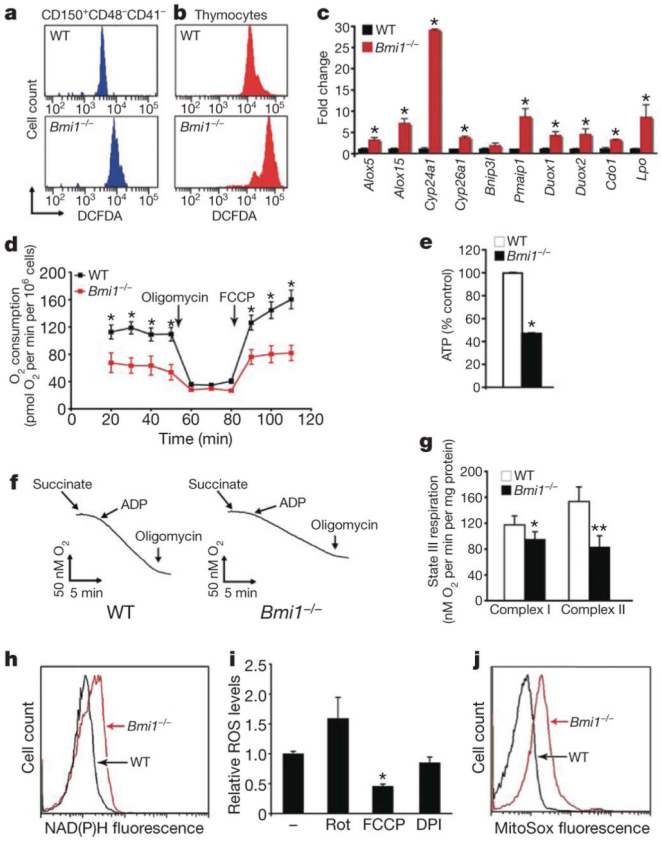

Figure 1. The absence of Bmi1 increases ROS levels and alters mitochondrial function

a, Levels of ROS as assessed by DCFDA fluorescence in purified wild-type (WT) or *Bmi1*$^{-/-}$ bone marrow cells. **b,** ROS levels in freshly isolated thymocytes. **c,** Quantitative rtPCR expression analysis of gene products involved in redox homeostasis in either WT or *Bmi1*$^{-/-}$ thymocytes. Results are normalized to *Gapdh* expression ($n = 3$ animals per group, $^{*}P < 0.05$). **d,** Oxygen consumption in intact thymocytes under basal conditions, following the addition of the mitochondrial inhibitor oligomycin (0.5 μg ml^{-1}) or in the presence of the uncoupler FCCP (1 μM). Cells were obtained from $n = 4$ animals per genotype; $^{*}P < 0.02$. **e,** Relative ATP levels in freshly isolated thymocytes. Measurements were made in triplicate (mean and s.d.) with 4 animals per group; $^{*}P < 0.01$. **f,** Representative oxygen consumption from isolated heart mitochondria. **g,** Measured state III respiration for either complex-I- or complex-II-dependent respiration (mean and s.d.; $n = 4$ animals per group; $^{*}P < 0.05$, $^{**}P < 0.01$). **h,** NAD(P)H levels as assessed by endogenous fluorescence in WT and *Bmi1*$^{-/-}$ thymocytes. **i,** ROS levels in *Bmi1*$^{-/-}$ thymocytes in the presence or absence of the complex I inhibitor rotenone (Rot), the chemical uncoupler FCCP or the NADPH oxidase inhibitor DPI (mean and s.d.; $n = 3$; $^{*}P < 0.05$). **j,** Analysis of thymocytes using the redox fluorophore MitoSox Red.

Author Manuscript Author Manuscript Author Manuscript Author Manuscript

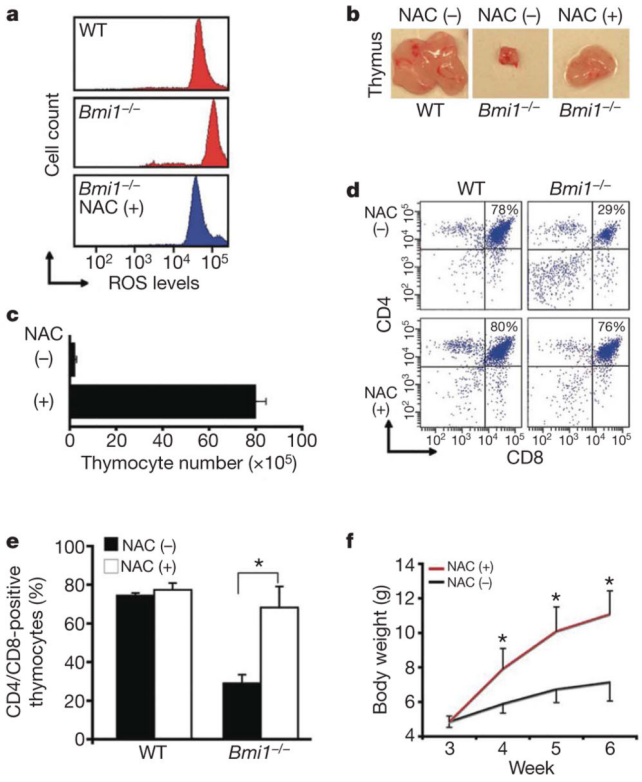

Figure 2. Antioxidant treatment rescues *Bmi1*$^{-/-}$ thymocytes

a, ROS in thymocytes isolated from four-week-old wild-type (WT) mice or *Bmi1*$^{-/-}$ mice randomized to NAC treatment for one week before collection. **b,** Overall thymus size in 4-week-old mice either treated for one week with NAC (+) of left untreated (–). **c,** Total number of thymocytes recovered in 4-week-old *Bmi1*$^{-/-}$ mice either treated for one week with NAC or left untreated (mean and s.d.; $n = 4$ animals per group). **d,** Representative assessment of thymocyte maturation ($CD4^+CD8^+$ cells) in 4-week-old WT or *Bmi1*$^{-/-}$ mice that were treated with NAC for one week or left untreated before collection. **e,** Quantitative assessment of thymocyte maturation in 4-week-old mice randomized for one week of antioxidant treatment (mean and s.d.; $n = 4$ animals per group). **f,** Weight of *Bmi1*$^{-/-}$ mice with or without antioxidant treatment beginning after weaning (mean and s.d.; $n = 5–7$ animals per group). *$P < 0.05$.

Author Manuscript Author Manuscript Author Manuscript Author Manuscript

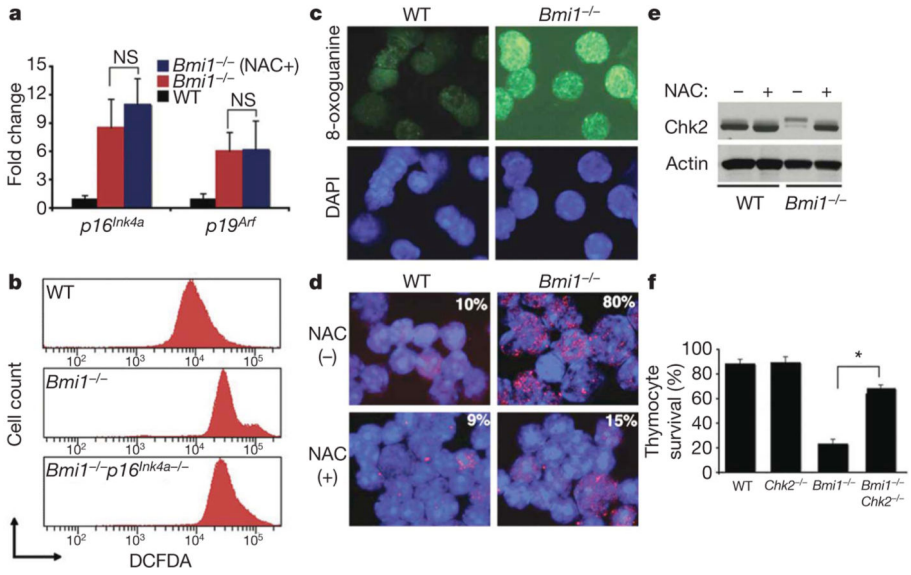

Figure 3. Activation of the DDR pathway in *Bmi1*$^{-/-}$ thymocytes occurs through a redox-sensitive pathway

a, Quantitative rtPCR analysis of *Ink4a/Arf* expression in thymocytes obtained from mice randomized to antioxidant therapy (mean and s.d.; n = 3 animals per group). NS, not significant. **b,** ROS levels in thymocytes obtained from WT, *Bmi1*$^{-/-}$ or combined *Bmi1/p16*^{Ink4a}-deleted mice. **c,** Levels of the oxidatively modified nucleotide 8-oxoguanine in isolated thymocytes. DAPI (4,6-diamidino-2-phenylindole) staining (blue) was used to visualize nuclei. **d,** 53BP1 nuclear foci thymocytes obtained from mice treated for one week before collection with the antioxidant NAC or left untreated. Overall percentage of thymocytes demonstrating activation of the DDR in each condition is shown. **e,** Western blot analysis for Chk2 activation in thymocytes obtained from WT or *Bmi1*$^{-/-}$ mice. **f,** Assessment of primary thymocyte survival in culture 24 h after isolation.

Author Manuscript Author Manuscript Author Manuscript Author Manuscript

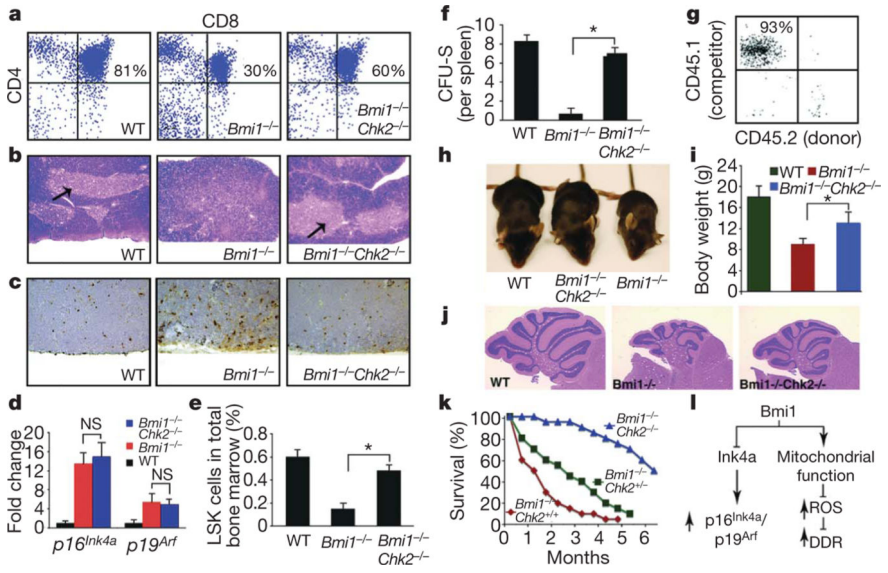

Figure 4. Inhibition of the DDR pathway by Chk2 deletion rescues multiple defects in *Bmi1*$^{-/-}$ mice

a, *Chk2* deletion restores *in vivo* thymocyte maturation of *Bmi1*$^{-/-}$ mice. WT, wild type. **b,** Architecture of the thymus in WT, *Bmi1*$^{-/-}$ and combined *Bmi1*$^{-/-}$*Chk2*$^{-/-}$ mice. The arrows point to a normal medulla region. **c,** Representative TUNEL staining in the cortex region of the thymus. **d,** Quantitative rtPCR analysis of *Ink4a/Arf* induction in *Bmi1*$^{-/-}$ or combined *Bmi1*$^{-/-}$*Chk2*$^{-/-}$ thymocytes (mean and s.d.; $n = 3$ animals per group). **e,** Frequency of LSK cells intotal bonemarrow (*$P < 0.01$; mean and s.d., $n = 6$ animals per group). **f,** *In vivo* CFU-S in lethally irradiated mice infused with equal numbers of bone marrow cells obtained from WT, *Bmi1*$^{-/-}$ or combined *Bmi1*$^{-/-}$*Chk2*$^{-/-}$ mice (*$P < 0.01$; mean and s.d., $n = 5$ animals per group). **g,** Peripheral blood composition four months after competitive repopulation in which equal amounts of WT competitor bone marrow cells (CD45.1) and combined *Bmi1*$^{-/-}$*Chk2*$^{-/-}$ donor bone marrow (CD45.2) were transplanted into an irradiated host (CD45.2). We observed little to no contribution of the donor-derived *Bmi1*$^{-/-}$*Chk2*$^{-/-}$ cells after such competitive repopulation experiments. **h,** Representative appearance of WT, *Bmi1*$^{-/-}$ or combined *Bmi1*$^{-/-}$*Chk2*$^{-/-}$ mice. **i,** Analysis of body weight at 6 weeks of age (*$P < 0.01$; mean and s.d.; $n = 6$ per group). **j,** Defects in cerebellar architecture observed in *Bmi1*$^{-/-}$ mice are rescued by Chk2 deletion. **k,** Lifespan of *Bmi1*$^{-/-}$ mice with varying Chk2 status. $P < 0.05$ *Chk2*$^{+/-}$ versus *Chk2*$^{+/+}$ and $P < 0.001$ for *Chk2*$^{-/-}$ versus *Chk2*$^{+/+}$; $n \geq 15$ animals per genotype. **l,** The Polycomb protein Bmi1 normally simultaneously represses the *Ink4a/Arf* locus leading to reduced p16^{Ink4a} and p19^{Arf} expression as well as modulating mitochondrial function to lower ROS levels and suppress activation of the DDR pathway. Activation of both Ink4a/Arf and the DDR have been separately linked to tumour suppression and stem cell ageing.